THE ASTROPHYSICAL JOURNAL, 275:461–466, 1983 December 15

VLBI OBSERVATIONS OF THE QSO 4C49.22

ROGER LINFIELD
Radio Astronomy Laboratory, University of California
Received 1983 March 14; accepted 1983 May 13

ABSTRACT

VLBI observations of the QSO 4C49.22 show a jet in P.A. 208° ± 3°, in the same direction as the innermost structure seen with the VLA. It is concluded that the kpc scale structure seen with the VLA is most likely due to a large-scale hydromagnetic instability in the jet. The lack of sub-kpc curvature suggests that the jet in this source has a smaller proper velocity $\gamma\beta$ (although it may still be relativistic), and a greater inclination to the line of sight, than in other extragalactic sources dominated by a compact core. A one-sided jet, which alternately flips 180°, is suggested by the observations.

Subject headings: interferometry — quasars

I. INTRODUCTION

A small fraction of extragalactic radio sources exhibit a multiply curved structure. Examples include the low-luminosity, type I (Fanaroff and Riley 1974) radio galaxies 3C31 and 3C449 (Fomalont *et al.* 1980; Perley, Willis, and Scott 1979), the head-tail galaxy 3C129 (Rudnick and Burns 1981), and the high-luminosity quasar 3C418 (Muxlow and Linfield 1983). The multiple bends seen in these sources suggest precessing jets (Gower and Hutchings 1983; Icke 1981; Muxlow and Linfield 1983), but alternatives have been proposed: gravitational encounters between the source of the jet and a companion object (Blandford and Icke 1978; Lupton and Gott 1982), and a helical hydromagnetic instability (Hardee 1981).

4C49.22, a QSO with $z = 0.334$, displays a multiply curved jet on a 2″–10″ scale, as seen in Figure 1 (Perley 1981). For $H_0 = 75$ km s^{-1} Mpc^{-1}, $q_0 = 0.5$, 1″ is subtended by 3.9 kpc. VLBI observations of the central object are reported in this paper.

II. OBSERVATIONS AND DATA REDUCTION

4C49.22 was observed on 1982 April 4–5 at 4.99 GHz with six telescopes; their locations, diameters, typical system temperatures, and antenna gains are given in Table 1. The Mark II recording system was used (Clark 1973), and the data were correlated at Caltech.

After being correlated, the data were run through a fringe-fitting program, and were then edited and calibrated to obtain correlated flux densities and closure phases. A model with three Gaussian components was obtained from the calibrated data by an iterative, least-squares procedure. This model reproduced the primary features of the data quite well. The model parameters are listed in Table 2. Because of a lack of short spacings in the *u-v* plane, the flux and size of the third component are not well constrained by the data. Only the approximate location (SW of the core) and orientation (~ N-S as opposed to E-W) are well established. In particular, the noncollinear nature of the model in Table 2 is not significant.

This model was used as input to a hybrid mapping procedure (Readhead and Wilkinson 1978). The resulting hybrid map is shown in Figure 2, and the fit of this map to the data is shown in Figure 3. The baselines and triangles in Figure 3 are those with a good signal-to-noise ratio, and on which the visibility function shows significant variation in amplitude/closure phase with GST. Because of imperfect amplitude calibration, particularly at Hat Creek, the dynamic range of the map shown in Figure 2 is limited to ~ 20:1. The dynamic range is too low to show the extended, low surface brightness emission to the SW of the core (component 3 in Table 2). The parameters of this component are best determined by model fitting.

From the model (Table 2) and hybrid map (Fig. 2) the following picture of the milli-arcsecond (mas) scale source structure emerges. There is an unresolved (< 0.3 mas diameter) component (the core), with an extension in P.A. 208° ± 3°. This extension has a fairly large ($\gtrsim 5$) aspect ratio, as determined by model fitting. This aspect ratio is not apparent from the hybrid map (Fig. 2) because of convolution with the restoring beam. The extension points directly at the innermost structure seen with the VLA, shown in Figure 1 (Perley 1981). Because of its large aspect ratio and its connection to the observed arcsecond jet, this mas extension will henceforth be called a jet.

A one-dimensional profile of the hybrid map (Fig. 2) along P.A. 208° is shown in Figure 4. The jet follows

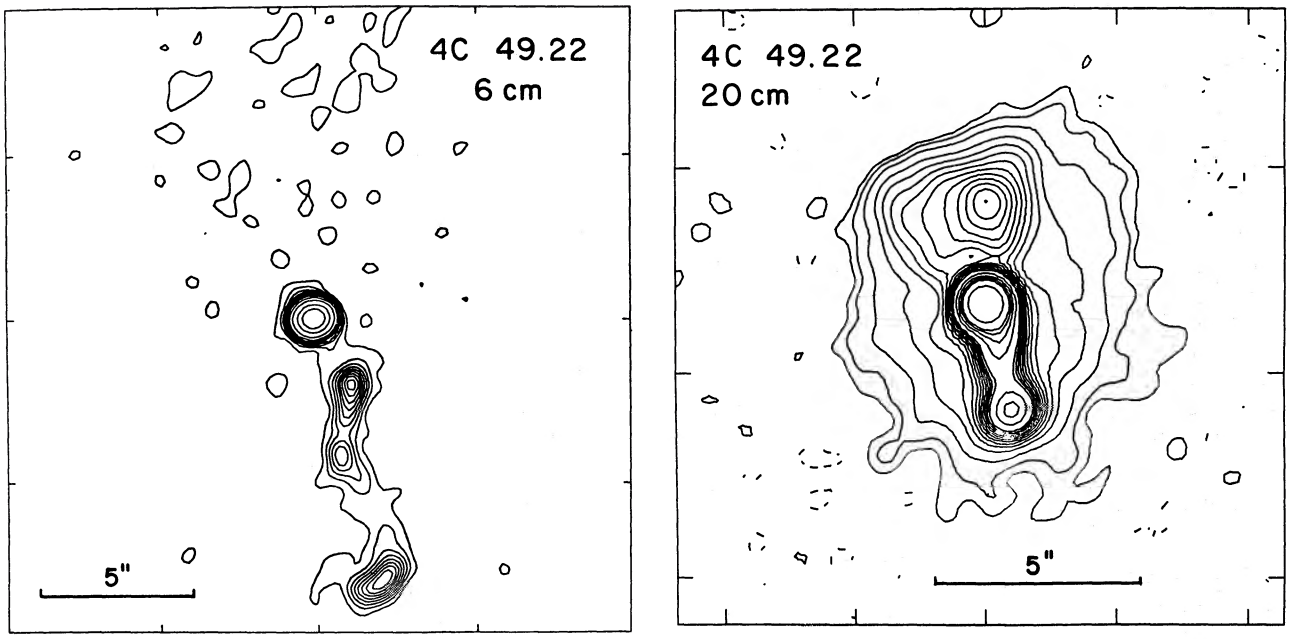

FIG. 1*a* FIG. 1*b*

FIG. 1.—VLA maps of 4C49.22 made by Perley (1981) and reproduced here with his permission. (*a*) 5.0 GHz, 0.7″ resolution, contour interval 0.33%, peak intensity 0.56 Jy per beam. (*b*) 1.5 GHz, 2″ resolution. Contour levels are −0.2%, 0.2%, 0.4%, 0.8%, 1.6%, 2.4%, 3.2%, 4.0%, 4.8%, 5.6%, 6.4%, 7.2%, 8.0%, 8.8%, 10%, 15%, 20%, 25%, 30%, and 50% of the peak intensity of 0.60 mJy per beam.

TABLE 1

TELESCOPE LOCATIONS AND PARAMETERS

Telescope Location	Diameter (m)	*K* (Jy)	Typical *T* (K)
Effelsberg, W. Germany ... (BONN)	100	1.40	60
Westford, MA ..... (HSTK)	37	0.16	75
Green Bank, WV..... (NRAO)	43	0.25	45
Fort Davis, TX ..... (FDVS)	26	0.094	55
Big Pine, CA ..... (OVRO)	40	0.20	110
Hat Creek, CA ..... (HCRK)	26	0.065	80

TABLE 2

4C49.22 SOURCE MODEL

COMPONENT	FLUX	DISPLACEMENT FROM COMPONENT 1		MAJOR AXIS FWHM	MINOR AXIS FWHM	
		d(mas)	P.A.	(mas)	(mas)	P.A.
1	0.33	0.	0.°	0.	0.	0.°
2	0.46	1.41	209.°	1.11	0.26	203.°
3	0.37	5.7	226.°	8.6	4.4	178.°
Beam				1.3	0.9	150.°

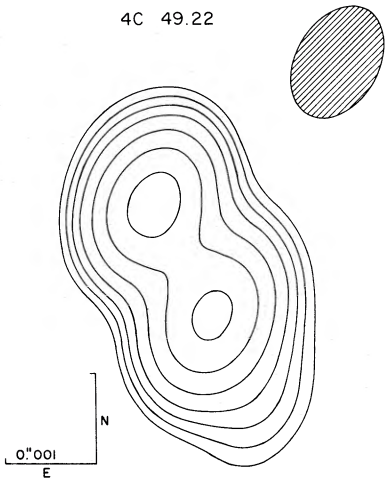

FIG. 2.—5.0 GHz hybrid map of 4C49.22 from six station VLBI observations. The beam is 1.31×0.90 mas, and the peak intensity is 0.23 Jy per beam. The contours are at 5%, 8%, 12%, 18%, 30%, 50%, and 80% of the peak. No negative contours appear at the −5% level. The crosshatched ellipse shows the half-power beam.

this P.A. for at least 3 mas; beyond this the P.A. is more weakly constrained by the data. From Figures 2 and 4 it can be seen that there is a prominent knot in the jet 1.39 ± 0.1 mas from the core. The core is unresolved on its NE side; there is no evidence for structure in this direction (i.e., a counterjet) on this scale. To the SW, the jet intensity increases rapidly until the knot, and then falls off more gradually; it disappears into the noise ~ 3 mas from the core. There is no evidence for systematic curvature on a mas scale. Small-amplitude wiggles on a scale < 0.8 mas or systematic curvature on a scale < 0.4 mas are not ruled out, however.

III. DISCUSSION

a) Implications of Arcsecond Curvature

The curvature in this source appears to occur almost entirely in the 2″–10″ range. If the curvature is due to precession, the period is

$$\tau \approx \frac{3 \times 10^6 \text{ yr}}{(1+z)\, v_{4_{\text{app}}}},$$

where

$$v_{4_{\text{app}}} = \frac{v_{\text{jet}} \sin\theta}{10^4 \text{ km s}^{-1} \left[1 - (v_{\text{jet}}/c)\cos\theta\right]},$$

and θ is the angle between the line of sight and the axis of the precession cone. Periods in this range can arise from the spin-orbit precession of a pair of massive (10^8–10^9 $M_\odot$) black holes (Begelman, Blandford, and Rees 1980). The quantities v_{jet}, θ, and ψ (the half-opening angle of the precession cone) are only weakly constrained by the available data, except that $\psi \approx 10° \sin\theta$.

There remains the problem of explaining the kpc-scale knots, both their existence and their location (at the bends in the jet). If the jet curvature is due to precession, possible causes include: time variations in the energy flow at the jet nozzle; shocks in the jet, presumably from interaction with gas clouds; interactions with the walls of a cavity evacuated by the jet; and time delay effects in a ballistic, precessing jet. The first two mechanisms could easily cause knots of the observed contrast, but there would be no tendency for these knots to occur at the observed bends in the jet. The third mechanism also suffers from this problem. A precessing jet possesses cylindrical symmetry; any anisotropy will be due to the environment, and should be uncorrelated with our line of sight. The fourth mechanism, in which knots form from purely kinematic effects in a ballistic precessing jet, has been investigated by Linfield (1981). When the flow velocity is relativistic, time delay effects across the precession cone distort its shape and alter the curvature. For a wide range of precession parameters, sharp bends occur at the edges of the precession cone, where jet material lies nearly along the line of sight. The jet intensity is strongly enhanced at these bends, as a result of increased optical depth. The edges of the precession cone are enhanced for a nonrelativistic jet also, but the effect is small unless the jet material forms a tight spiral. This model provides a natural explanation for the location of the knots in 4C49.22, but cannot produce the high contrast knots close to the core that this source possesses (Linfield 1981).

If the curvature is not due to precession, jet material is bent after it leaves the nozzle. If the observed curvature arises from pressure bending or hydromagnetic instabilities, bright knots are expected to form at the bends in the jet, as a result of interaction with the walls of the transport tube. Unlike in the precession case, the bends correspond to the regions of greatest actual curvature. Neither these processes nor precession can explain the mas knot; it must arise from other causes (e.g., time variations in nuclear activity). Pressure gradients can bend jets, but the shape of 4C49.22 would demand a very exotic spatial pressure distribution. Hydromagnetic instabilities are a more likely cause. The magnetic field plays a major role in such instabilities, whether the jet is thermally or magnetically confined. The field in 4C49.22 is parallel to the jet in its interior (Perley, private communication); the field outside the jet is unknown.

Ray (1981) has studied the Kelvin-Helmholtz stability of jets confined by thermal pressure. For Mach number $\mathcal{M} \gtrsim 3$ (probably the case for 4C49.22), pinching modes ($m = 0$) grow slowly. Helical modes ($m = 1$) grow more

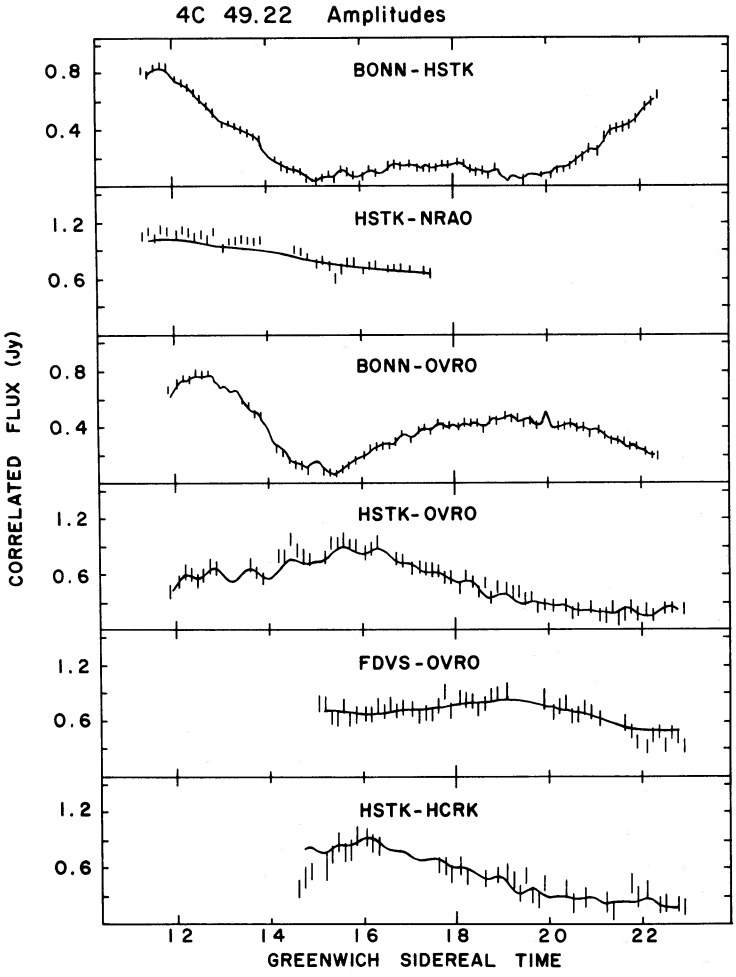

FIG. 3*a*

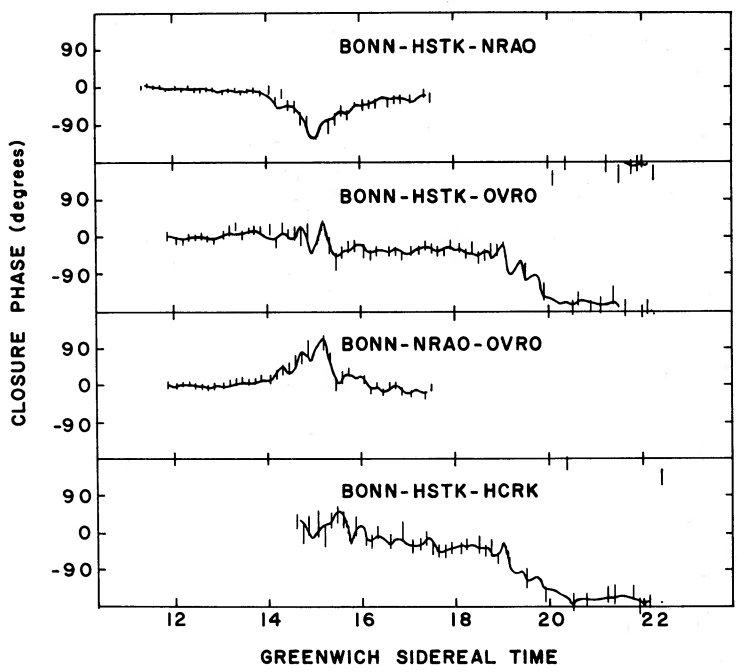

FIG. 3*b*

FIG. 3.—4C49.22 VLBI data vs. GST on selected baselines and triangles (see text). Solid lines correspond to the map in Fig. 2 (prior to convolution with the restoring beam). (*a*) Correlated flux densities. (*b*) Closure phases.

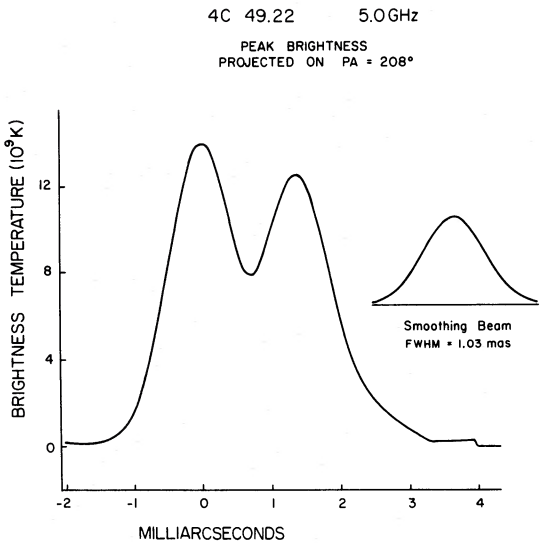

FIG. 4.—Profile of 4C49.22 along P.A. 208

rapidly, but are suppressed by an axial magnetic field. An axial field whose internal energy is comparable to the jet kinetic energy is sufficient to stabilize the $m=1$ modes.

The case of a jet confined by its own magnetic field has been investigated by Cohn (1983); his results will be used here because his assumptions most closely reflect the conditions thought to hold in 4C49.22. He assumed an azimuthal field generated by a surface current; the return current was taken to be at a large distance ($\gg r_{\rm jet}$) from the jet axis. For simplicity, he assumed zero internal field and solved only the pinching modes ($m=0$). For $3r_{\rm jet} < \lambda < 30r_{\rm jet}$ the growth rates are comparable to the sound speed crossing time. For the static case, the growth rates for the $m=0$ and $m=1$ modes are comparable, and both are slowed or inhibited by an axial magnetic field (Chandrasekhar, Kaufman, and Watson 1958). If the growth rates for the pinch and kink ($m=1$) modes are comparable in the nonstatic case as well, the time for a small perturbation to grow to large amplitude is

$$\tau_{\rm growth} \equiv 10\times 20\times \frac{1}{{\rm Im}(\omega)} \approx 3f\left(\frac{\mathscr{M}}{5}\right)\tau_{\rm flow}\sin i,$$

where Im(ω) is the imaginary part of the complex perturbation frequency ω, f is the factor by which the axial magnetic field reduces the growth rate, $\tau_{\rm flow}$ is the length of time for material to flow down the jet ($\tau_{\rm flow} = l_{\rm jet}/\mathscr{M} c_s$), and i is the inclination of the jet to the line of sight; $l_{\rm jet} \approx 30r_{\rm jet}$. For $f=3$, $\mathscr{M}=5$, $c_s = 1200$ km s^{-1}, and $\sin i = 1$, $\tau_{\rm growth} \approx 7\times 10^7$ yr. If the shape of the jet is due to a hydromagnetic instability, the perturbation has reached a large amplitude. The curvature is now sufficiently large that if the perturbation is still growing, the jet may be on the verge of being completely disrupted.

The disruption of the jet would release a large quantity of plasma into the interstellar medium in a turbulent manner. Outward diffusion at the Alfvén speed ($B/[4\pi\rho]^{1/2}$) would create a low surface brightness cocoon around the former location of the jet. Such a cocoon is seen in the low-resolution VLA map (Fig. 1*b*). It is present on both sides of the core, but is much brighter and wider to the north of the core. It extends roughly equal distances from the core in both directions.

The presence of the bright cocoon to the north suggests the prior existence of a jet in that direction. This jet is not currently visible, even on a mas scale, suggesting that its source of supply has been off for $\tau > \tau_{\rm flow}$. Like other radio sources (Lonsdale 1981), 4C49.22 shows evidence for a one-sided jet which alternates directions. An approximate lower limit to the flipping time is the growth time calculated above. If the cocoon has reached its current lateral extent of 50 kpc radius in 7×10^7 yr by outward diffusion at the Alfvén speed, the magnetic field is $3n_{-4}^{1/2}$ μG, where $n_{-4} = n/10^{-4}$ cm^{-3}. The synchrotron lifetime is shorter than this diffusion time unless $n_{-4} < 0.01$, but even mild particle acceleration, driven by the kinetic energy of the outflow, would suffice to keep the cocoon lit.

The cocoon is present to the south of the core, but is weaker and more irregular than to the north. This may be a relic from a southern jet which disrupted $> 2\tau_{\rm growth}$ in the past, if the alternating jet hypothesis holds for this source.

b) Implications of the Lack of Sub-Arcsecond Curvature

4C49.22 fits neatly into the "core" source category of Readhead, Cohen, and Pearson (1978) (asymmetric overall structure, centimeter flux dominated by a very compact component, projected size <100 kpc), except for the lack of sub-arcsecond curvature. Sources such as 3C273 and 3C345 show a continuous P.A. change of 20°–50° from the sub-mas level to the arcsecond level. This large observed curvature is generally ascribed to a projection effect, with the jet forming a small angle to the line of sight. The lack of observed curvature in 4C49.22 could imply (1) the bending occurs almost entirely in a plane containing the line of sight, (2) the intrinsic curvature is negligible, or (3) the inclination is a substantial fraction of a radian, so that the curvature is not strongly amplified.

If the above arguments for a jet instability explanation of the arcsecond bends are correct, the jet velocity is subrelativistic (or perhaps mildly relativistic) on a kpc scale. This, in turn, argues against a large (~ 10) γ-factor on a mas scale, since this would require an enormous ($\pi\gamma\rho_j r_j^2 c^3 \approx 10^{47}$–$10^{48}$ ergs s^{-1}) energy dissipation in the inner few kpc. A low-γ jet would be likely to be

observed at a moderate to large inclination (20°–60°) because of its broad Doppler-beaming cone.

IV. CONCLUSIONS

4C49.22 has the peculiar combination of a dominant core, one-sided structure, little or no sub-kpc scale curvature, and multiple bends on a kpc scale. The following deductions are made about the source:

1. Precession is unable to produce the observed kpc-scale jet appearance.

2. A more likely cause is a Kelvin-Helmholtz or kink mode instability. Such instabilities may completely disrupt the jet on a time scale of ~ 3–10×10^7 yr, accounting for both the strong asymmetry and the low-brightness cocoon surrounding the jet.

3. The observations are consistent with an intrinsically one-sided jet, which flips on a time scale $\sim 10^8$ yr.

4. The inclination of the jet to the line of sight may well be substantially greater than the small ($i < 10°$) values generally estimated for "core" sources. As such, 4C49.22 may be intermediate in jet velocity and inclination between typical "core" sources such as 3C345, and extended sources such as Cyg A.

I thank D. Backer and J. Arons for helpful discussions. R. Perley kindly supplied unpublished polarization VLA maps of this source. An anonymous referee made several useful suggestions. The National Radio Astronomy Laboratory is operated by Associated Universities, Inc., under contract with the National Science Foundation. This work was supported in part by NSF grant AST81-14717.

REFERENCES

Begelman, M. C., Blandford, R. D., and Rees, M. J. 1980, *Nature*, **287**, 307.
Blandford, R. D., and Icke, V. 1978, *M.N.R.A.S.*, **185**, 527.
Chandrasekhar, S., Kaufman, A. N., and Watson, K. M. 1958, *Proc. Roy. Soc. London, A.*, **245**, 435.
Clark, B. G. 1973, *Proc. IEEE*, **61**, 1242.
Cohn, H. 1983, *Ap. J.*, (in press)
Fanaroff, B. L., and Riley, M. 1974, *M.N.R.A.S.*, **167**, 31P.
Fomalont, E. B., Bridle, A. H., Willis, A. G., and Perley, R. A. 1980, *Ap. J.*, **237**, 418.
Gower, A. C., and Hutchings, J. B. 1982, *Ap. J.* (*Letters*), **258**, L63.
Hardee, P. E. 1981, *Ap. J.* (*Letters*), **250**, L9.
Icke, V. 1981, *Ap. J.* (*Letters*), **246**, L65.
Linfield, R. 1981, *Ap. J.*, **250**, 464.
Lonsdale, C. 1981, Ph.D. thesis, University of Manchester.
Lupton, R. H., and Gott, J. R., III. 1982, *Ap. J.*, **255**, 408.
Muxlow, T. W. B., and Linfield, R. P. 1983, in preparation.
Perley, R. A. 1981, ESA SP-162, pp. 77–81.
Perley, R. A., Willis, A. G., and Scott, J. S. 1979, *Nature*, **281**, 437.
Ray, T. P. 1981, *M.N.R.A.S.*, **196**, 195.
Readhead, A. C. S., Cohen, M. H., and Pearson, T. J. 1978, *Nature*, **276**, 768.
Readhead, A. C. S., and Wilkinson, P. N. 1978, *Ap. J.*, **223**, 25.
Rudnick, L., and Burns, J. O. 1981, *Ap. J.* (*Letters*), **246**, L69.

ROGER LINFIELD: 264-748, Jet Propulsion Laboratory, 4800 Oak Grove Drive, Pasadena, CA 91103